

## An Investigation of the Input Impedance of a Microstrip Probe in Waveguide.

S. Withington and G. Yassin

*Department of Physics,  
University of Cambridge,  
Madingley Rd, Cambridge.*

### Abstract

We derive an expression for the input impedance of a one-sided microstrip probe in waveguide. By "one-sided" we mean an insulated probe that extends only part way across the waveguide. This arrangement contrasts with the "Eisenhart and Kahn" or "double-sided" configuration, where the probe extends the whole way across the waveguide and is earthed at both ends. Our analysis is based on the spectral-domain method and is able to take into account the dielectric substrate on which the thin-film antenna is deposited. In submillimetre-wave components, the thickness of the substrate is 10-20% of the width of the waveguide, and the substrate has a significant effect on performance. We have examined the validity of our model by carrying out extensive impedance measurements at 5GHz. A key feature of the paper is that we compare the general characteristics of the one-sided probe, in the context of SIS mixers, with those of the two-sided probe. We show that the bandwidth of a probe that stretches only part way across the waveguide is very much greater than the bandwidth of a probe that stretches all of the way across the waveguide. Moreover, the input resistance is lower and more suited to SIS tunnel junctions. We also show, analytically, that the input impedance is almost independent of axial orientation.

## I Introduction

Waveguide-mounted superconducting tunnel junctions have been used as mixers in low-noise submillimetre-wave receivers for many years. It is usual practice to couple the tunnel junction to the waveguide by locating it at the centre of a thin, conducting strip which extends the whole of the way across the waveguide and which is earthed at both ends. As the demands on the technology grow, however, it is important to ask whether this arrangement is optimum or whether some other arrangement would be more effective. In particular, we are interested in getting the greatest possible bandwidth out of the waveguide to tunnel-junction transition, and in extending the frequency of operation to above 1THz where conventional waveguide becomes small and difficult to manufacture.

The double-sided probe, which was analysed rather elegantly by Eisenhart and Khan [1], is known to be effective, but has the disadvantage that it is not possible to obtain low values of input impedance ( $50\ \Omega$  or less) without significantly reducing the height of the waveguide—even when an adjustable backshort tuner is used. As we shall see later, this property is intrinsic to the Eisenhart and Khan configuration, and is a consequence of the fact that the device is most naturally described by an input admittance. That is to say, the contributions from the scattered evanescent modes add up in parallel and influence the real part of the input impedance in a complicated way. In the one-sided probe, however, the contributions from the scattered evanescent modes add up in series, and only the propagating fundamental mode couples to the resistive part of the input impedance. As a consequence, the input impedance is relatively independent of frequency and is straightforward to control.

In a previous paper we developed an expression for the input impedance of a free-standing, one-sided microstrip probe [2]. In this paper we include in the model the dielectric substrate on which the thin-film antenna is deposited. In submillimetre-wave components the dielectric can occupy a significant fraction of the waveguide and must therefore be taken into account. We verify the integrity of the theory by performing a range of experiments, at 5GHz, on a scale model. At the end of the paper, we compare the general characteristics of one-sided probes and two-sided probes in the context of submillimetre-wave SIS

mixers.

The full-wave analysis of a probe in a waveguide is not an easy problem. The task is particularly complex if one wants to take into account the field radiated by the aperture through which the feeding transmission line passes—clearly, this additional complexity does not arise in the case of the Eisenhart and Khan probe. Despite the complications, Collin [3] has provided a solution, based on the *space-domain* dyadic Green's function, for the input impedance of a cylindrical probe in a rectangular waveguide. First he employed the method of moments, in conjunction with Galerkin's technique, to derive a general expression for the input impedance of a probe; then he performed substantial analytical manipulations to get a fast numerical algorithm. A similar approach, based on the method of moments, has also been used to calculate the input impedance of a microstrip probe [4]. In this case, however, the conventional Galerkin method, which results in a large matrix equation where each matrix element is found by double integration, was employed. This method requires a great deal of computing time even though the supporting dielectric substrate is not taken into account.

In this paper, we develop further the basic technique reported by Ho and Shih [5] to produce an expression for the input impedance of a microstrip probe. The approach is based on the reciprocity theorem and the spectral-domain method. An important feature of the theory is that the Fourier transforms of the current and field distributions are related—through the *spectral* dyadic Green's function—by an algebraic rather than an integral equation. Moreover, the expression for the spectral Green's function is much simpler and easier to obtain than the space-domain version—especially for dielectrically-loaded waveguide. The spectral-domain approach also has the advantage that modal properties of the dielectrically-loaded probe are brought out clearly, and we can determine how thick the substrate can be before higher-order modes introduce resonant features into the input impedance.

To verify the validity of the theory, we carried out extensive measurements on a scale model. A frequency range of 4-6GHz was chosen in order to scale the operation of a 450-500GHz mixer block by a factor of a 100. We measured the complex input impedance of a variety of different probes—various lengths, widths, and backshort locations.

Such data is surprisingly rare in the literature, and in most cases only the return loss is given, which is not sufficient to provide a sensitive test of the theories. To isolate the behaviour of the probe from that of the probe-backshort combination, we measured the input impedance of the probe with both ends of the waveguide terminated with matched loads.

## II Basic Theory

In Fig. 1, we show the geometry of a microstrip probe. The probe is assumed to be fed by a current source  $I_{in}$  which is connected between the base of the probe and the wall of the waveguide. This source causes a potential difference  $V_{ab}$  to be established, through which the input impedance of the probe can be defined according to

$$Z_{in} = \frac{V_{ab}}{I_{in}} \quad (1)$$

Using the reciprocity theorem [6],[7], we can derive an expression for  $V_{ab}$  in terms of the current density on the surface of the probe  $J_x$  and the tangential electric field in the waveguide  $E_x$ ; in this way, we obtain the expression

$$Z_{in} = -\frac{1}{I_{in}^2} \int \int \int E_x(r) J_x(r) dV \quad (2)$$

When evaluating the above integral we assume that the current is distributed sinusoidally over the length of the probe. This assumption allows a great deal of simplification and eventually leads to an elegant solution for the input impedance. It is nevertheless also possible to obtain the real current distribution as a bi-product of the solution of a full-wave numerical analysis by expanding  $J_x$  in terms of a set of basis functions and then calculating the coefficients of the expansion by using standard iterative techniques. Experimental results show that the use of a simple one-term expression is sufficient for most practical purposes. We therefore write

$$J_x(x, y, z) = J_0 \delta(y - d) u(z) \sin k(x_1 - x) \quad (3)$$

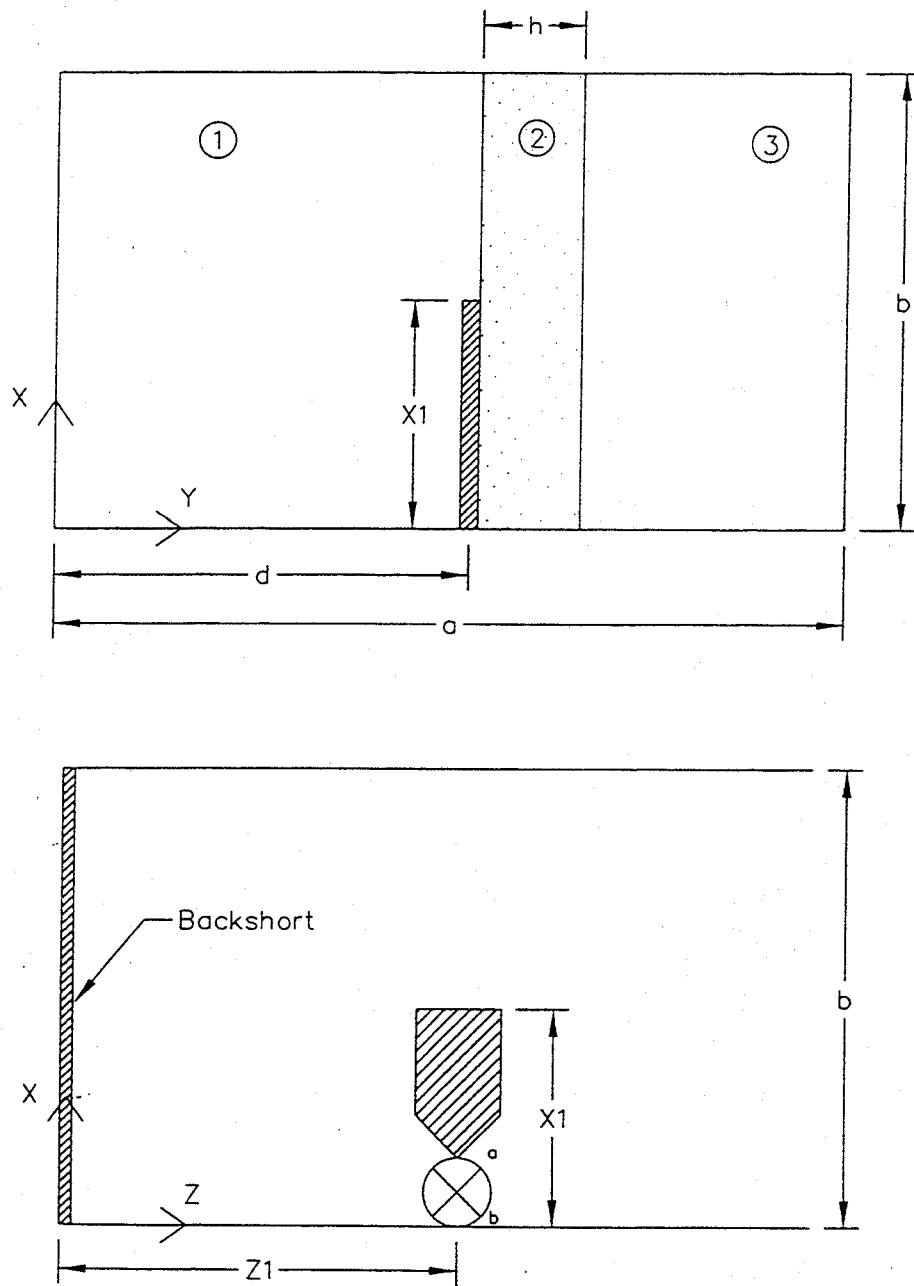


Figure 1: A microstrip probe.

for  $x < x_1$  and zero otherwise.  $u(z)$  describes the current density distribution across the width of the probe and can be written as

$$u(z) = \frac{1}{\pi} \frac{1}{\sqrt{1 - \left(\frac{z-z_1}{w}\right)^2}} \quad |z - z_1| < w, \quad (4)$$

where  $w$  is the half width of the probe. Notice that in the first instance we are assuming that the plane of the probe is in the E-plane of the waveguide: we shall call this type of probe a 'longitudinal probe' as distinct from a 'transverse probe' where the plane of the probe is transverse to the direction of propagation. In the following treatment, we shall neglect the transverse components of the current  $J_z$  and the electric field  $E_z$ .

To apply the spectral-domain method to our problem we first replace the current and field in (2) by their Fourier transforms and apply Parseval's theorem in three dimensions to obtain

$$Z_{in} = -\frac{1}{2\pi b} \frac{1}{I_{in}^2} \sum_{n=-\infty}^{+\infty} \sum_{m=-\infty}^{+\infty} \int_{-\infty}^{+\infty} \tilde{E}_x(\alpha, \gamma, \beta) \tilde{J}_x(\alpha, \gamma, \beta) d\beta \quad (5)$$

where

$$\tilde{J}_x(\alpha, \gamma, \beta) = (2j) \sin \frac{m\pi d}{a} J_0(|\beta w|) \left[ \frac{k}{k^2 - \alpha^2} (\cos \alpha_n x_1 - \cos kx_1) \right]. \quad (6)$$

To derive the above expression we Fourier transformed the current distribution of (3) by using the method of images. In addition, boundary conditions on the field distributions require

$$\alpha_n = \frac{n\pi}{b}. \quad (7)$$

The input impedance can now be calculated by using the spectral-domain relationship between the current and field distributions. Neglecting the transverse component of the field and current, which we find to be justified experimentally, we obtain

$$\tilde{E}_x(\alpha, \gamma, \beta) = \tilde{G}_{xx}(\alpha, \gamma, \beta) \cdot \tilde{J}_x(\alpha, \gamma, \beta) \quad (8)$$

where

$$\tilde{G}_{xx}(\alpha, \gamma, \beta) = \frac{\alpha^2}{\alpha^2 + \beta^2} Z^e + \frac{\beta^2}{\alpha^2 + \beta^2} Z^h. \quad (9)$$

Here  $\bar{G}_{xx}(\alpha, \gamma, \beta)$  is the longitudinal component of the dyadic Green's function.  $Z^e$  and  $Z^h$  are the Green's functions associated with the LSE and LSM modes. According to the scheme we can take into account the presence of the supporting dielectric substrate merely by using the appropriate Green's function. Substituting (6) in (5) and using the residue theorem we can now obtain an expression for the input impedance:

$$Z_{in} = \frac{j}{kb} \sum_{n=0}^{+\infty} \delta_n \sum_{m=1}^{+\infty} \lim_{\beta \rightarrow \beta_{mn}} \left\{ \left( \frac{\beta - \beta_{mn}}{k} \right) \left[ J_0(\beta w) \left( \sin \frac{m\pi d}{a} \right) \left( \frac{\cos \alpha_n x_1 - \cos kx_1}{\sin kx_1} \right) \right]^2 \left( \frac{k^2}{k^2 - \alpha_n^2} \right)^2 \cdot \tau_{mn}(\beta) \cdot \bar{G}_{xx}(\alpha_n, \gamma, \beta) \right\}. \quad (10)$$

In the above equation,  $\beta_{mn}$  are the poles of  $\bar{G}_{xx}$  which satisfy the relation

$$\beta_{mn}^2 = k^2 + \gamma_m^2 - \alpha_n^2 \quad (11)$$

and  $\delta_n = \begin{cases} 1 & \text{for } n=0 \\ 2 & \text{otherwise} \end{cases}$ . Also  $\tau_{mn}(\beta)$  is the reflection coefficient of the termination at  $z=0$ . It can be written as

$$\tau = \begin{cases} 2j \sin \beta z_1 \exp -j\beta z_1 & \text{for a lossless backshort} \\ 1 & \text{for a matched termination} \end{cases} \quad (12)$$

Equation (10) gives the input impedance of a microstrip probe that lies in the E-plane of a rectangular waveguide. This equation applies to all dielectric thicknesses and all probe locations.

An important case, which can be treated by the above theory, is the free-standing planar probe; that is to say we ignore the dielectric substrate. In this case, the Green's function is given by

$$\bar{G}_{xx}(\alpha, \gamma, \beta) = \frac{jR_0}{\gamma/k} \left[ \frac{1 - \alpha_n^2}{k^2} \right] \left( \frac{\sinh^2 \gamma d}{\sinh \gamma a} \right). \quad (13)$$

Computing the limit yields  $\gamma_m = jm\pi/a$ , and the input impedance of the probe becomes

$$Z_{in} = -\frac{2jR_o}{k^2ab} \sum_{n=0}^{+\infty} \sum_{m=1}^{+\infty} (-1)^m \delta_n \left[ J_o(\beta w) \left( \sin \frac{m\pi d}{a} \right)^2 \left( \frac{\cos \alpha_n x_1 - \cos kx_1}{\sin kx_1} \right)^2 \times \frac{\sin \beta_{mn} z_1}{\beta_{mn}/k} \frac{e^{-j\beta_{mn} z_1}}{[1 - (\alpha_n/k)^2]} \right] \quad (14)$$

where the propagation constant is now simply

$$\beta_{mn} = \left[ k^2 - \left( \frac{m\pi}{a} \right)^2 - \left( \frac{n\pi}{b} \right)^2 \right]^{1/2} \quad (15)$$

$k$  is the propagation constant of free space,  $R_o$  is the impedance of free space, and  $J_o$  is the ordinary Bessel function.

At this stage, before the dielectric is included in the model, it is instructive to compare (14) with the equivalent expression derived by Eisenhart and Khan for the input impedance of a probe which extends the whole way across the waveguide and which is earthed at both ends. Assuming a gap of width  $2g$  and taking into account the presence of the backshort, we obtain [1]

$$Z'_{in} = \left( \sum_{n=0}^{+\infty} \frac{1}{Z_n} \right)^{-1} \quad (16)$$

where

$$Z_n = \frac{jR_o b}{a} \sum_{m=1}^{+\infty} \frac{1}{\delta_n} \left[ \frac{\text{sinc}(|\gamma_m|w) \sin(\frac{m\pi d}{a})}{\text{sinc}(\alpha_n g) \cos(\frac{n\pi h}{b})} \right]^2 \times [1 - (\alpha_n/k)^2] \frac{\sin \beta_{mn} z_1}{\beta_{mn}/k} e^{-j\beta_{mn} z_1} \quad (17)$$

and  $h = b - 2g - x_1$ :  $h$  and  $x_1$  are the distances from the edges of the gap to the walls of the waveguide. Comparing (14), (16) and (17) we notice that the two expressions have some striking similarities. In particular, in each case the total input impedance consists of a combination of elemental impedances, where the elemental impedances essentially reflect the fact that energy is either stored or dissipated by each of the



$TE_{mn}$  and  $TM_{mn}$  waveguide modes. In contrast, however, in the case of the microstrip probe, the terms add up in series, whereas in the case of the Eisenhart and Kahn probe the terms add up in parallel. Consequently, for the microstrip probe the real part of the input impedance is due solely to the lowest-order propagating mode; whereas for the Eisenhart and Khan probe, the real part of the input impedance is influenced by the large number of high-order non-propagating modes. This basic and important difference results in the Eisenhart and Khan probe being characterised by a high value of input impedance whereas the microstrip probe is characterized by a relatively low value of input impedance. Moreover, the input impedance of the two-sided probe has a complicated frequency dependence. In order to reduce the input impedance of the Eisenhart and Kahn probe, and to increase the bandwidth, the height of the waveguide is usually reduced by a factor of about 4, but this modification increases the conduction losses and the manufacturing complexity—both of which are extremely important if one wants to manufacture components for the THz frequency range.

We can now write the final design equations for the input impedance,  $Z_{in} = R_{in} + jX_{in}$ , of a free-standing microstrip probe in single-moded waveguide as

$$R_{in} = \frac{2R_o}{k\beta_{1o}ab} \tan^2\left(\frac{kx_1}{2}\right) \sin^2(\beta_{1o}z_1) J_o^2(\beta_{1o}w) \sin^4\left(\frac{\pi d}{a}\right) \quad (18)$$

$$X_{in} = X_{10} + \frac{2R_o}{k^2ab} \left[ \sum_{m=2}^{\infty} X_{m0} + \sum_{n=1}^{+\infty} \sum_{m=1}^{+\infty} X_{mn} \right] \quad (19)$$

$$X_{10} = \frac{R_o}{k\beta_{1o}ab} \tan^2\left(\frac{kx_1}{2}\right) \sin 2(\beta_{1o}z_1) J_o^2(\beta_{1o}w) \sin^4\left(\frac{\pi d}{a}\right) \quad (20)$$

$$X_{mn} = -(-1)^m \delta_n \left[ J_o(|\beta_{mn}|w) \left( \sin^2 \frac{m\pi d}{a} \right) \left( \frac{\cos \alpha_n x_1 - \cos kx_1}{\sin kx_1} \right) \right]^2 \\ \times \frac{\sinh |\beta_{mn}|z_1}{|\beta_{mn}|/k} \frac{e^{-|\beta_{mn}|z_1}}{[1 - (\alpha_n/k)^2]} \quad (21)$$

where  $X_{10}$  is the inductive contribution of the propagating mode and  $X_{mn}$  is the expression inside the double summation (14). It is interesting to notice that for  $w \rightarrow 0$ , (18) becomes identical to Collin's formula for the input resistance of a coaxial probe[8].

A question often asked is ‘what happens to the input impedance of a planar probe when it is rotated about its axis?’ Clearly, some device configurations will favour the longitudinal probe whereas other device configurations will favour the transverse probe. The above theory can easily be modified to cover the situation where the probe is transverse to the direction of propagation. First we imagine that the current distribution in the  $x - z$  plane, at  $y = d$ , is given by

$$J_x = J_0 \sin k(x_1 - x) \delta(z_1) u(y) . \quad (22)$$

The corresponding electric field can be obtained through the spectral-domain method in exactly the same way as before, and then the terms in the expression for the input impedance are modified as follows:

$$Z_{mn}|_{\text{Transverse}} = \left\{ \frac{J_0(|\gamma_m w|)}{J_0(|\beta_{mn}|)} \right\}^2 Z_{mn}|_{\text{Longitudinal}} . \quad (23)$$

It is interesting to notice that the difference between the input impedance of the longitudinal probe and the input impedance of the transverse probe is very small. We therefore conclude that the orientation of the probe can be chosen for mechanical convenience alone.

Having now discussed the general properties of probes by considering the free-standing case, we would like to include the supporting dielectric substrate. Moreover, we would like to make the modification to the longitudinal probe because the longitudinal probe is the most useful configuration for ‘split-block’ technology [9]. We can calculate the input impedance of the new geometry by using (10) and inserting the Green’s function for a three-layer dielectric system. This modification is straightforward to make in the spectral-domain because the transverse resonance technique can be used to derive  $\bar{G}_{xx}(\alpha_n, \gamma, \beta)$ . Applying the immittance method [10] we find that

$$Z^e = \frac{y_2 C t_3 + y_3 C t_2}{C t_2 C t_3 + C t_1 C t_3 y_2 / y_1 + C t_1 C t_2 y_3 / y_1 + y_3 / y_2} \quad (24)$$

and

$$Z^h = \frac{z_2 C t_2 + z_3 C t_3}{z_1 z_2 C t_1 C t_2 + z_1 z_3 C t_1 C t_3 + z_2 z_3 C t_2 C t_3 + z_2^2} \quad (25)$$

where

$$C t_1 = \coth \gamma_1 d, \quad C t_2 = \coth \gamma_2 h, \quad C t_3 = \coth \gamma_3 a - (d + h) ; \quad (26)$$

also

$$y_i = \frac{\gamma_i}{j\omega\epsilon_i}, \quad z_i = \frac{\gamma_i}{j\omega\mu} \quad (27)$$

where the subscript denotes the region of the cross section, 1,2 or 3, under consideration, see Fig. 1.

Numerically, a difficult aspect of evaluating the impedance is finding the transverse propagation constant  $\gamma$ . Although one is simply finding the roots of the transcendental equations derived through the transverse resonance method (or equivalently the poles of the Green's function) subject to the auxiliary conditions

$$\beta_{mn}^2 = k_i^2 + \gamma_{mi}^2 - \alpha_n^2, \quad (28)$$

for all  $i$ , the problem is complicated because the system is three-layered and poles and closely-spaced roots exist. It is therefore a little awkward to ensure that all of the roots and poles are found and that the poles are removed. It turns out to be much more straightforward to perform this task if one assumes that the dielectric is placed symmetrically in the waveguide and the transverse-resonance equations are simplified accordingly. We have found, for geometries of practical interest, that the results are almost identical to the more complicated case when one places the dielectric slightly off axis. In all cases, however, we use a current distribution which is on-axis regardless of whether or not we approximate the off-axis Green's function with the on-axis Green's function. In general terms, an important feature of the method is that the transverse resonance equations lead to a clear understanding of the modes that can propagate in the dielectrically-loaded section of the waveguide, and this has important implications for the bandwidths of probes, as we shall see later.

### III Experimental Results and Discussion

To investigate the above theory, we manufactured a scale model of a 400-500GHz mixer block. The waveguide had dimensions of  $a=47\text{mm}$  and  $b=22\text{mm}$ , and the probe was fed by an SMA connector which was inserted into the centre, ( $d = a/2$ ), of the broad wall. The central conductor of the SMA connector penetrated 0.5mm into the waveguide and a copper-foil probe was soldered to the end. The dielectric

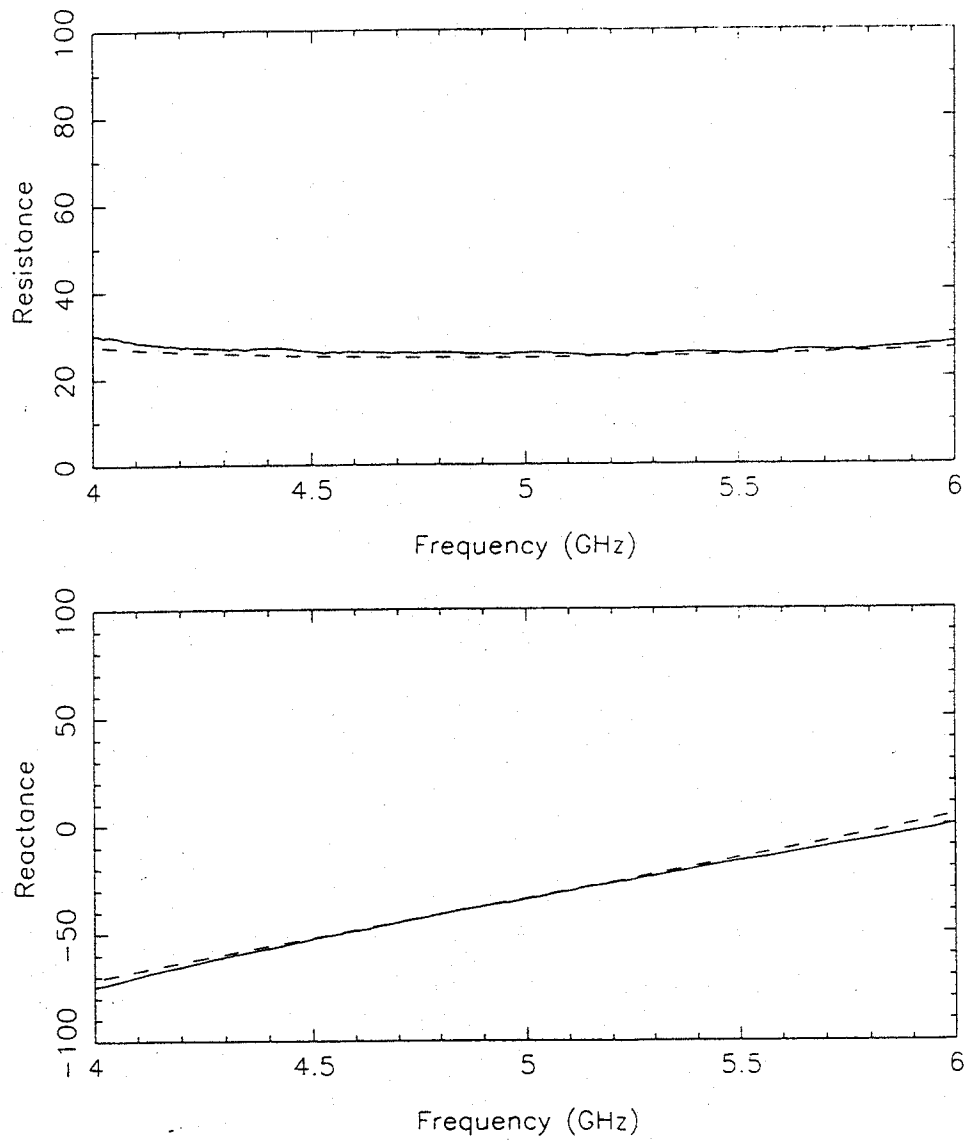


Figure 2: The input impedance of a doubly-matched microstrip probe as a function of frequency. The probe was orientated in the longitudinal direction, no dielectric was used,  $w = 3\text{mm}$ , and  $x_1 = 12\text{mm}$ . The dotted lines correspond to the experimental data and the solid lines to the theoretical model.

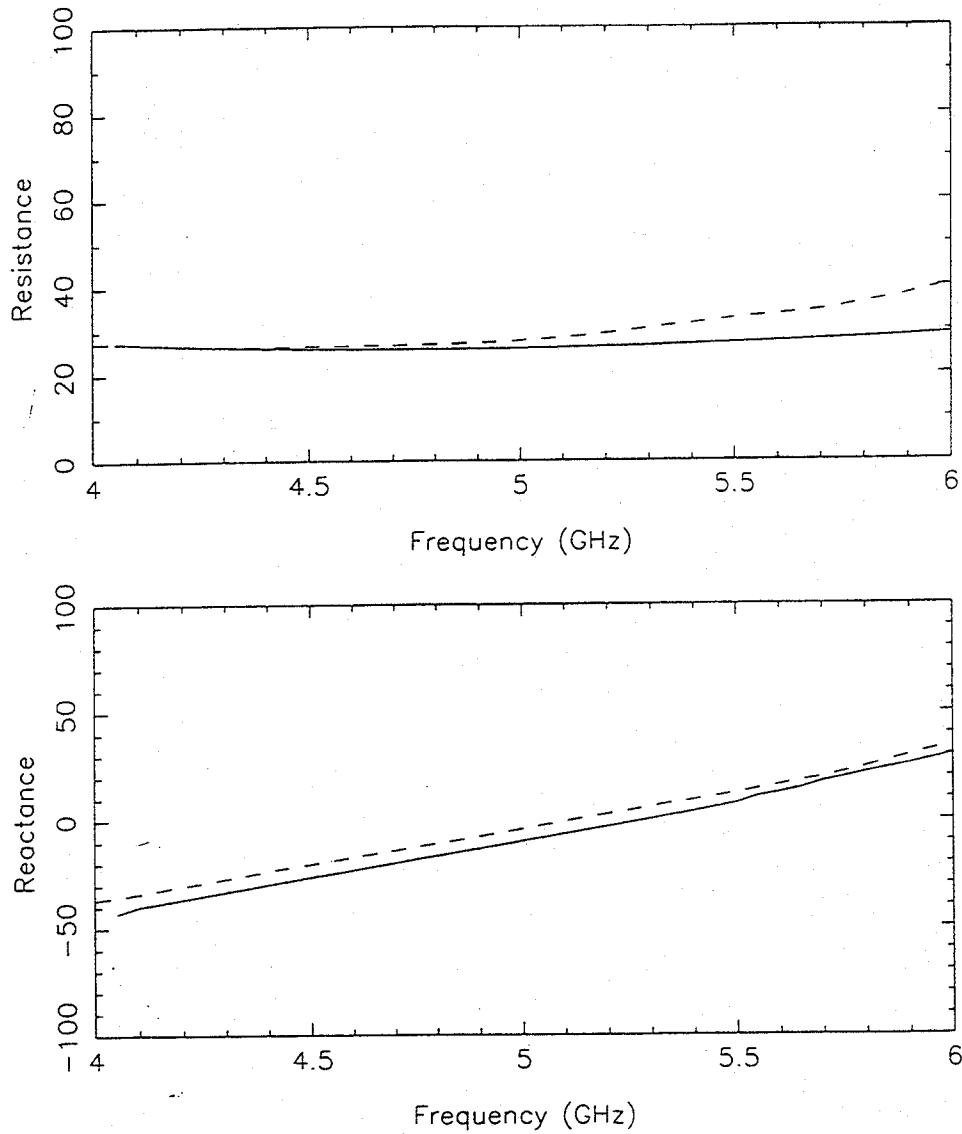


Figure 3: The input impedance of a doubly-matched microstrip probe as a function of frequency. The probe was orientated in the longitudinal direction, the PTFE dielectric was 7mm thick,  $w = 3\text{mm}$ , and  $x_1 = 12\text{mm}$ . The dotted lines correspond to the experimental data and the solid lines to the theoretical model.

was 7mm thick and was made out of PTFE. Originally, we attempted to use Nylon 66 because its dielectric constant is similar to that of quartz. Unfortunately, however, although the reactive part of the input impedance agreed well with theory, the real part was higher than predicted and this seems to have been due to the known high losses in Nylon 66. To remove the effects of reflections from the ends of the dielectric we tapered the substrate over a distance of approximately 100mm. In addition, we verified the effectiveness of the tapers by measuring the return loss, without a probe but with the dielectric, looking into one end of the waveguide with the other terminated with a match load. The reflections from the ends of the substrate were at a level of below -15dB. A major advantage of the arrangement described here is that a short circuit can be applied at the wall of the waveguide in order to establish a well-defined reference plane for the impedance measurements. It is substantially more difficult to do well-calibrated impedance measurements on an Eisenhart and Kahn probe.

In order to separate out the intrinsic behaviour of the probe from that of the probe-backshort combination, we terminated both ends of the waveguide with matched loads. The real and imaginary parts of the input impedance were then measured by using a Vector Network Analyser. In Fig. 2 we show the input impedance of a doubly-matched probe as a function of frequency. In this case the probe was 3mm wide and 12mm long and no dielectric was included. In Fig. 3 we show the input impedance when a 7mm thick PTFE substrate was included. Firstly, it can be seen that theory and experiment agree extremely well in both cases. Secondly, it can be seen that the dielectric does influence the behaviour of the probe even in the case where the dielectric is relatively thin compared to the width of the waveguide and the dielectric constant is low. More specifically, the real part of the impedance is changed very little, but the imaginary part changes significantly. The difference occurs of course because the imaginary part is determined by local, non-propagating modes, whereas the real part is determined by non-local propagating modes. An important observation is that the microstrip probe is essentially a low-impedance structure with a typical input resistance in the range 10-60 $\Omega$ . This range is ideally suited to the characteristic impedances of microstrip lines. From the point of view of SIS mixers, the probe can be used for

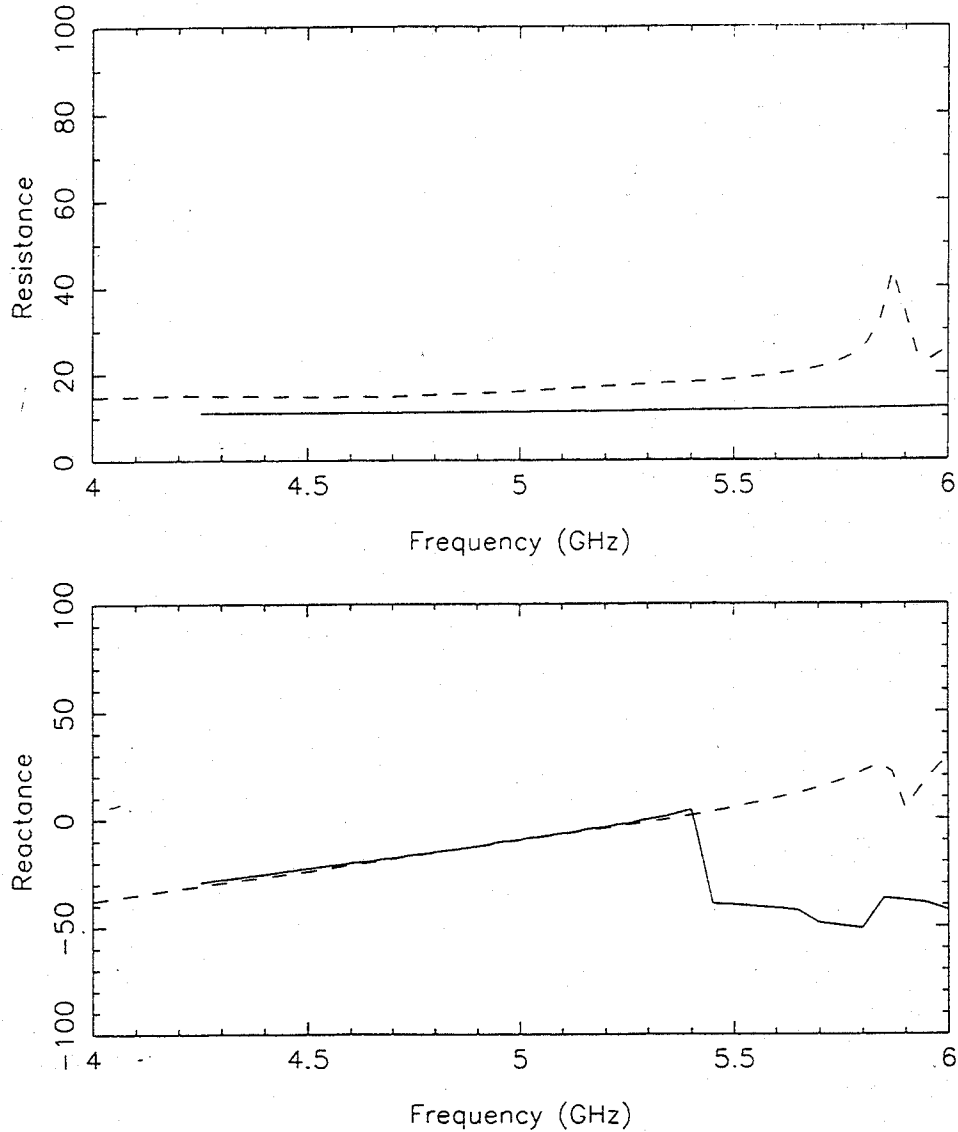


Figure 4: The input impedance of a doubly-matched microstrip probe as a function of frequency. The probe was orientated in the longitudinal direction, the Nylon 66 dielectric was 7mm thick,  $w = 3\text{mm}$ , and  $x_1 = 9\text{mm}$ . The dotted lines correspond to the experimental data and the solid lines to the theoretical model.

feeding SIS tunnel junctions over broad frequency ranges without the need to reduce the height of the waveguide [11].

An important observation when performing the experiments was that for dielectric constants of 3.8, high-order modes can start to propagate in the dielectric-loaded waveguide, over the frequency range considered, in addition to the lowest-order LSE and LSM modes. This leads to a stronger dependence on frequency than one would like. The effect is shown in Fig. 4 where Nylon 66 has been used in place of PTFE. The theoretical model cuts off at a frequency of 5.4 GHz due to the onset of high-order modes—although we could include them in the model if desired—and the experimental data shows a peak due to a resonance between high-order modes. In the context of mixers this means that as the substrate is made thicker the bandwidth of the probe is reduced. This behaviour and the frequency at which it occurs is fully predicted and can be understood by means of our theory. In fact we find, for practical mixers, that high-order modes in the probe are more influential in determining the bandwidth than high-order modes in the IF channel [12]. Another notable feature of Fig. 4 is that experiment and theory do not agree when one looks at the real part of the impedance, but they do agree when one looks at the reactive part. We believe that this effect is due to the very high microwave losses that are known to be associated with Nylon 66.

#### IV Conclusions

We have derived an expression for the input impedance of a microstrip probe in waveguide. In the case where the dielectric is extremely thin and can be neglected, the expression can be reduced to a very simple analytical form. In the case where the dielectric is taken into account, the expression is more complicated but straightforward to evaluate numerically. A major advantage of developing a theory of this kind, over simply relying on three-dimensional electromagnetic simulators, is that one gets a clear understanding of the underlying physics involved.

Our work on microstrip waveguide probes leads us to the following conclusions:

1. For the two-sided probe the effects of the propagating and non-propagating modes add up in parallel leading to a high input



impedance with a narrow bandwidth. This is intrinsic to the structure and can only be overcome by reducing the height of the waveguide. For the one-sided probe the impedances associated with the individual modes add up in series leading to a low-impedance broadband structure. In fact only the lowest-order propagating mode makes a contribution to the real part of the input impedance.

2. With the one-sided probe a low-impedance broad-band structure can be made without reducing the height of the waveguide. In fact for THz operation it may well be possible to use oversized waveguide.
3. For the one-sided probe we have shown that the axial orientation of the film has very little influence on the input impedance, meaning that the orientation can be chosen for mechanical convenience alone. To our knowledge this is the first time that this effect has been proven theoretically.
4. When a supporting dielectric substrate is included, the modal behaviour becomes more complicated and it is necessary to keep the substrate thinner than some certain value to avoid resonances and achieve broad-band operation. Normally, one keeps the substrate thin to avoid high-order modes in the IF filter and not to avoid high-order modes in the probe. In practice it seems that the probe dictates how thick the substrate should be.

In summary, we feel that a well-designed one-sided probe is better than a two-sided probe.

#### References

- [1] R.L. Eisenhart and P.J. Khan, "Theoretical and experimental analysis of a waveguide mounting structure," *IEEE Trans. Microwave Theory Tech.*, vol. MTT-19, pp. 706-717, 1971.
- [2] G. Yassin and S. Withington, "Analytical expression for the input impedance of a microstrip probe in waveguide," *Int. J. Infrared Millimeter Waves*, vol. 17, pp. 1685-1705, 1996.

- [3] R.E. Collin, *Field Theory of Guided Waves*, IEEE Press: New York, pp. 471-483, 1991.
- [4] F. Chen and W. B. Dou, "Full-wave analysis of a waveguide-to-microstrip transition for millimeter wave applications," *Int. J. Infrared and Millimeter Waves*, vol. 16, pp. 641-652, 1995.
- [5] T.Q. Ho and Yi-Chi Shih, "Spectral-domain analysis of E-plane waveguide to microstrip transition," *IEEE Trans. Microwave Theory Tech.*, vol. MTT-37, pp. 388-392, 1989.
- [6] W.L. Weeks, *Electromagnetic Theory for Engineering Applications*, John Wiley & Sons, Inc.: New York, 1964.
- [7] V.H. Rumsey "Reaction concept in electromagnetic theory," *Phys. Rev.*, vol. 94, pp. 1483-1491, 1954.
- [8] R.E. Collin, *Field Theory of Guided Waves*, McGraw-Hill: New York, 1960.
- [9] S. Withington, G. Yassin, M. Buffey, and C. Norden, "A horn-reflector antenna for high-performance submillimetre-wave imaging arrays," *Int. J. Infrared and Millimeter Waves*, vol. 18, pp. 341-358, 1997.
- [10] T. Uwano and T. Itoh, "Spectral Domain Approach," in *Numerical Techniques for Microwave and Millimeter-Wave Passive Structures*, Ed. T. Itoh, John Wiley & Sons, New York, 1989.
- [11] A.R. Kerr and S.-K. Pan, "Some recent developments in the design of SIS mixers," *Int. J. Infrared Millimeter Waves*, vol. 11, pp. 1169-1187, 1990.
- [12] S. Withington and G. Yassin, "Spectral-Domain Analysis of Submillimetre-Wave Microstrip Filters," *Int. J. Infrared and Millimeter Waves*, vol. 14, pp. 1975-1984, 1993.